A new organically-templated cobalt borophosphate with a novel borophosphatic anionic partial structure

Wei Liu*, Xiang-Qin Guo, Ge Su, Li-Xin Cao, Yong-Gang Wang, Jing-Rui Duan

Institute of Material Science and Engineering, The Ocean University of China, Qingdao 266100, PR China

ABSTRACT

A novel cobalt borophosphate, $(NH_4)_2(C_4H_{12}N_2)[Co_2B_4P_6O_{24}(OH)_2] \cdot H_2O$ with the mixed cations has been synthesized under mild hydrothermal conditions. Its crystal structure was determined by the single-crystal X-ray diffraction (tetragonal, $I4_1/a$ (no. 88), $a=14.207(3)$ Å, $c=24.956(6)$ Å, $V=5037.09(2)$ Å^3, $Z=8$). The crystal structure consists of a new type of three-dimensional borophosphatic anionic partial framework, which is built from the condensation of the fundamental building unit (FBU) $[B_2P_3O_{14}(OH)]$. The CoO_6 octahedra are enclased in such borophosphate network to form a complex open framework with a three-dimensional intersecting channel system, the voids of which are occupied by ammonium, dipronated piperazine ions and water molecules, respectively. The magnetic measurement of the title compound has also been investigated.

© 2011 Elsevier Inc. All rights reserved.

1. Introduction

The compounds with open-framework structures are of great interest from both the industrial and academic point of view due to their applications as catalysts, ion-exchangers, or molecular sieves [1,2]. Structurally similar to silicates, aluminosilicates, and aluminophosphates, metal borophosphates as a relatively young research field have drawn much attention in the past decade and a large number of new compounds with various dimensionalities and stoichiometries have been reported [3–11]. Particularly, the hydro-/solvothermal synthetic techniques in the presence of organic templates have greatly extended this family since the first organio-borophosphate $Co(C_2H_{10}N_2)[B_2P_3O_{12}(OH)]$ was reported in 1997 [12–16]. According to the principles and fundamental building units (FBUs) proposed by Kniep et al., the frameworks of the borophosphates can be featured by various anionic partial structures, such as oligomeric units, chains, ribbons, layers, and three-dimensional (3D) open frameworks [17]. In compared to the numerous low-dimensional anionic partial structures, the 3D anionic partial structures of the borophosphates are rare. To our best knowledge, there are only nine examples with the 3D borophosphatic anionic structures including $NH_4[BPO_4F]$ [18], $M[B_2P_2O_8(OH)]$ ($M=$Rb, Cs) [19], $A[BeBP_2O_8] \cdot H_2O$ ($A=$Na, K, NH_4) [20], $KMBP_2O_8$ ($M=$Sr, Ba) [21], $(NH_4)_4[B_2P_4O_{14}(OH)_2]$ [22], $CsFe[BP_3O_{11}]$ [23], $Na_2[VB3P_2O_{12}(OH)] \cdot 2.92H_2O$ [24], $Na_8[Cr_4B_{12}P_8O_{44}(OH)_4][P_2O_7] \cdot nH_2O$ [25] and $(NH_4)_6[Mn_3B_6P_9O_{36}(OH)_3] \cdot 4H_2O$

[26] so far. Here we report the first cobalt borophosphate $(NH_4)_2(C_4H_{12}N_2)[Co_2B_4P_6O_{24}(OH)_2] \cdot H_2O$ with the 3D anionic partial borophosphatic network prepared by the introduction of the mixed templates of NH_4^+ and piperazine under hydrothermal conditions.

2. Experimental section

2.1. General

The reagents used were commercially obtained with analytical purities and used without further purification. The products were examined by the X-ray diffraction (Rigaku D/max 2550 V diffractometer, Cu$K\alpha$) in order to confirm their phase identity and purity. The elemental analysis was performed on ICP-AES (Vista AX ICP-AES). IR spectra were collected on a Digilab-FTS-80 spectrophotometer from 4000 to 400 cm^{-1} using pressed KBr pellets of the samples. Thermogravimetric analysis and differential scanning calorimetry (TGA and DSC) were performed using a STA-409PC/4/H LUXX DSC-TGA instrument at a heating rate of 10 K/min in a air flow from the room temperature to 1073 K. The magnetic susceptibility measurements were carried out with a SQUID magnetometer (Quantum-Design, MPMS XL-7) in the temperature range of 2–300 K.

2.2. Synthesis and characterizations

In a typical synthesis, CoO, $NH_4HB_4O_7 \cdot 3H_2O$, piperazine and deionized water were mixed in the molar ratio 2:2.5:10:667, and

* Corresponding author.
  E-mail address: weiliu@ouc.edu.cn (W. Liu).

then the amount of 3 mL of H_3PO_4 (85 wt%) was gradually added to adjust the pH at 3.0–4.0. The solution was then transferred to a Teflon-lined stainless steel autoclave and was heated at 473 K for 5 days under autogenetic pressure. The pink rod crystals were separated by the vacuum filtration, washed thoroughly with deionized water and ethanol, and finally dried at 333 K in air. Its experimental XRD pattern (Fig. S1) was in agreement with the simulated one generated on the basis of the single-crystal structural data, proving the phase purity of as-synthesized products. The ICP-AES elemental analysis was used for Co, B, and P, while a hot-extraction method was applied for the analysis of carbon and nitrogen. The observed (calculated) mass (%): Co, 13.15(12.99); B, 4.78(4.76); P, 21.42(20.51); C, 5.57(5.29); N, 6.28(6.17). The IR spectrum of the title compound is shown in Fig. S2. Vibration modes for B–O and P–O are observed at 1187, 1029, 975, 925, 848, 640, 566 cm^{-1}. The peak at 3428 cm^{-1} corresponds to the bending vibrations of O–H, and the peaks at 3097 and 1623 cm^{-1} are attributed to the stretching and bending vibrations of the NH_4^+ groups. Additional absorption bands for C–C, C–N, N–H and C–H bending and stretching vibrations are observed at 1307–3235 cm^{-1}, which confirm the presence of protonated piperazine molecules. Thermogravimetric analysis showed three steps of the mass loss (Fig. S3). The weight loss between 313 and 353 K is 1.9% and is in agreement with the removal of the water molecules from the channels (calcd 1.9%). No weight loss is observed after this step up to 723 K. A total mass loss of 14.5% in the range of 723–833 K with an endothermal peak corresponds to the removal of the ammonium and piperazine molecules (calcd 14.3%). Further mass loss of 1.9% occurs above 833 K and it is consistent with the removal of one molar equiv of water through the condensation of the OH groups (calcd 2.0%).

2.3. Crystal structure determination

Crystals of the title compound were selected under a polarizing microscope, glued to a thin glass fiber with cyanoacrylate (superglue) adhesive, and inspected for singularity. The data sets were collected at 295 K on a Nonius Kappa CCD diffractometer equipped with a normal focus, 2.4 kW sealed tube X-ray source (Mo$K\alpha$ radiation, $\lambda=0.71073$ Å) operating at 50 kV and 40 mA. The structures were solved in the space group $I4_1/a$ (no. 88) by the direct methods using the program SHELXS-97-2 [27]. Fourier calculations and subsequent full-matrix least-squares refinements were carried out using SHELXL-97-2. Additional information about the data collection and structure refinement is presented in Table 1. The cobalt, phosphor atoms were located form the structure solution, whereas the oxygen, boron, carbon, and nitrogen atoms were found in the difference Fourier maps.

3. Results and discussion

3.1. Crystal structure

The asymmetric unit of the title compound contains one crystallographically unique Co site, two unique B sites and three unique P sites (Fig. 1). Both B atoms are in the tetrahedral coordination with the B–O bond lengths ranging from 1.411(6) to 1.484(6) Å. The condensation of B(1)O₄ and B(2)O₄ groups via one bridging oxygen leads to the B_2O_7 binuclear group. Of four distinct P sites, P(1) and P(2) atoms are tetrahedrally coordinated by four O atoms, forming the PO_4 tetrahedron geometry with the P–O bond distances ranging from 1.487(6) to 1.574(6) Å. The P(3) atom is coordinated by three O atoms and one protonated oxygen. The Co atoms are octahedrally coordinated by six oxygen atoms with the Co–O bond lengths ranging from 2.064(6) to

Table 1
Crystal data and structure refinements for $(NH_4)_2(C_4H_{12}N_2)$ $[Co_2B_4P_6O_{24}(OH)_2]\cdot H_2O$.

Empirical formula	$C_4H_{24}B_4Co_2N_4O_{27}P_6$
Formula weight	907.11
Wavelength (Å)	0.71073
Temperature (K)	295
Crystal system	Tetragonal
Space group	$C4_1/a$
a (Å)	14.207(3)
b (Å)	14.207(3)
c (Å)	24.956(6)
V (Å³)	5037.1(18)
Z	8
D_{calc} (g cm⁻³)	2.384
μ(Mo$K\alpha$) (mm⁻¹)	1.843
θ range (deg.)	1.55–50.0
Total data collected	10,004
Unique data	2113
F	3568
S	1.092
R indices[$I > 2\sigma(I)$], R_1, wR_2	0.078, 0.145
Final R indices, R_1^α, wR_2^α	0.127, 0.164

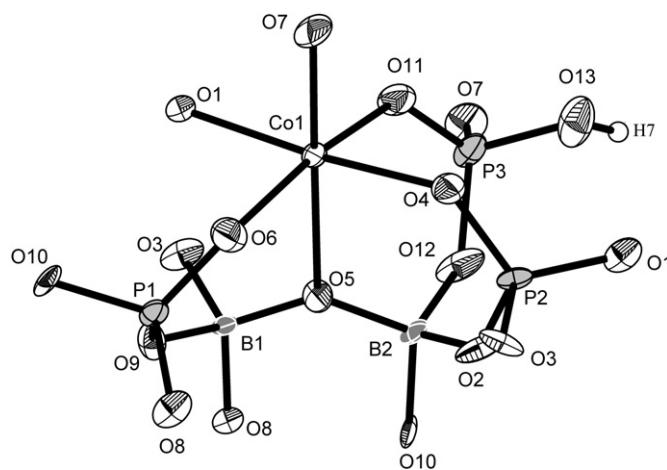$w=1/[\sigma^2(F_O)^2+(0.0882P)^2]$, where $P=[F_O^2+2F_C^2]/3$.

Fig. 1. The thermal ellipsoid plots (50% probability) and atomic labeling schemes of the framework in the title compound.

2.135(6) Å. Five of these oxygen atoms are shared by nearby P atoms and the sixth oxygen is connected with two B atoms. The selected bond distances and angles are given in Table 2.

The crystal structure of the title compound is featured by a structural building cluster containing one CoO_6 octahedron, one $[B_2O_7]$ binuclear unit, three PO_4 tetrahedra and one $PO_3(OH)$ tetrahedron (Fig. 2 inset). Such building clusters are connected through sharing PO_4 tetrahedra to form the complex channel system of the title compound. The one-dimensional opening along the c-axis are constructed by three types of eight-membered polyhedral rings with the topological sequences of CoO_6–PO_4–BO_4–PO_4–CoO_6–PO_4–BO_4–PO_4 (A); CoO_6–PO_4–CoO_6–PO_4–CoO_6–PO_4 (B) and BO_4–PO_4–BO_4–PO_4–BO_4–PO_4 (C), respectively. As shown in Fig. 2, the overlap of such polyhedral rings in the sequence of $ABAC$ gives rise to the formation of this 1D channel with a square-like opening. The aperture size of the channel is around 5.92×5.92 Å² (O–O distance). The channels exhibit the motif of a tetragonal rod packing along the c-axis. The more complex porous structure can be observed along the a and b axes, respectively (Fig. 3). Similar to the channels along the c-axis, these openings can also be described by the overlap of the eight-membered polyhedral rings. Besides known A and B types,

Table 2
Selected bond distances (Å) and angles (deg.) for $(NH_4)_2(C_4H_{12}N_2)[Co_2B_4P_6O_{24}(OH)_2] \cdot H_2O$.

Co1—O7	2.064(6)	P3–O12	1.560(6)
Co1-O11[(i)]	2.067(6)	P3–O13	1.574(6)
Co1-O6	2.104(6)	B1–O5	1.411(11)
Co1-O4	2.098(6)	B1–O3	1.469(11)
Co1-O1	2.116(6)	B1–O8[(iii)]	1.481(11)
Co1-O5	2.135(6)	B1–O9	1.484(11)
P1–O6	1.487(6)	B2–O5	1.436(10)
P1–O9	1.546(6)	B2–O2[(iv)]	1.446(11)
P1–O10	1.534(6)	B2–O12[(i)]	1.460(11)
P1–O8	1.537(6)	B2–O10[(iii)]	1.478(10)
P2–O1	1.490(6)	N2–C2B[(iv)]	1.48(3)
P2–O4[(ii)]	1.509(6)	N2–C1	1.544(17)
P2–O2	1.563(6)	N2–C2A	1.55(2)
P2–O3	1.566(6)	C1–C2A[(vii)]	1.31(2)
P3–O11	1.486(6)	C1–C2B[(viii)]	1.32(2)
P3–O7	1.491(8)		
O7–Co1–O11[(i)]	99.5(2)	O11–P3–O13	107.3(4)
O11[(i)]–Co1–O6	169.7(2)	O7–P3–O13	108.1(4)
O7–Co1–O4	84.6(2)	O5–B1–O3	113.9(7)
O6–Co1–O4	92.9(2)	O3–B1–O8[(iii)]	104.5(7)
O4–Co1–O1	175.1(2)	O5–B1–O9	109.9(7)
O4–Co1–O5	90.0(2)	O8[(iii)]–B1–O9	105.4(7)
O6–P1–O9	112.6(3)	O5–B2–O2[(iv)]	112.6(7)
O6–P1–O10	112.5(3)	O2[(iv)]–B2–O12[(i)]	111.1(7)
O9–P1–O8	107.4(3)	O5–B2–O10[(iii)]	112.2(7)
O10–P1–O8	105.7(3)	O12[(i)]–B2–O10[(iii)]	106.5(8)
O1–P2–O2	110.9(3)	C2B[(iv)]–N2–C1	108.8(12)
O1–P2–O3	108.5(3)	C1–N2–C2A	115.3(11)
O4[(ii)]–P2–O3	110.1(3)	C2A[(vii)]–C1–N2	119.8(15)
O2–P2–O3	103.9(3)	C2B[(viii)]–C1–N2	112.7(12)
O11–P3–O7	115.2(3)	C1[(vii)]–C2A–N2	111.0(15)
O7–P3–O12	108.2(3)	C1[(ix)]–C2B–N2[(ii)]	114.6(16)

(i) 0, 0, 0; (ii) $-y$, 0.5+x, 0.25+z; (iii) 0, 0, 0; (iv) $-1-x$, $-y$, $-1+z$; (vii) y, $1-x$, $-z$; (viii) $-y$, x, $-1-z$; (ix) $-1+x$, 0.5+y, 0.25−z.
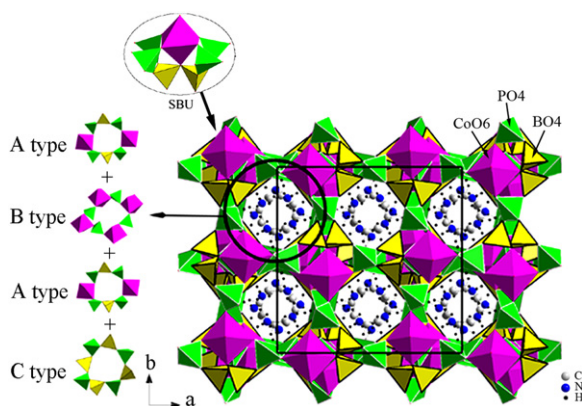

Fig. 2. Details of the crystal structure of the title compound viewed in [001] direction. (PO4 tetrahedron, green; BO4 tetrahedron, yellow; CoO6 octahedron, pink; carbon, gray sphere; nitrogen, blue sphere; hydrogen, small black sphere). (For interpretation of the references to color in this figure legend, the reader is referred to the web version of this article.)

there exists a new eight-membered ring with the topological sequence of CoO_6–PO_4–CoO_6–PO_4–CoO_6–PO_4–BO_4–PO_4 (D). All of them repeat themselves along the a or b axis, respectively, to form three type channels, which are arranged alternately and interconnected to form the complex channel systems.

The intersection of these channels produces two types of cavities, where ammonium, dipronated piperazine cations and water molecules are located, respectively (Fig. 4). One cavity built from eight-membered polyhedral rings contains a pair of ammonium cations and one water molecule (Fig. 4a), which connect with the anionic
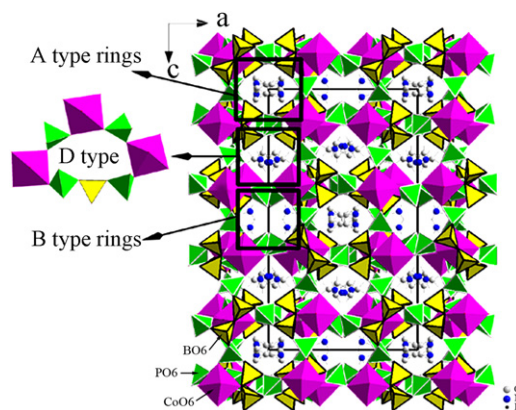

Fig. 3. Details of crystal structure of the title compound viewed along [010] direction. (PO4 tetrahedron, green; BO4 tetrahedron, yellow; CoO6 octahedron, pink; carbon, gray sphere; nitrogen, blue sphere; hydrogen, small black sphere). (For interpretation of the references to color in this figure legend, the reader is referred to the web version of this article.)

framework via hydrogen bonds (N1–H1⋯O11, N1–H2⋯O2, N1–H3⋯O10, N1–H4⋯O11). The dipronated piperazine molecules in the crystal structure suffer from a conformational disorder, which causes two equivalent positions of carbon atoms C(2) with the refined occupancies of 50%. Located in the other cavity built from three- and eight-membered polyhedral rings, these organic dications are fixed via the hydrogen bond interactions formed between the ammine groups of the amine dications and the oxygen atoms of the anions (N2–H5⋯O6, N2–H6⋯O9) (Fig. 4b). According to the classification of organic–inorganic compounds mentioned by Cheetham et al., the title compound would classified as I^3O^0 (metal–ligand–metal=0 and inorganic connectivity=3) [28].

As few examples of metal borophosphates with 3D anionic partial structures, the title compound features a novel borophosphate 3D anionic partial framework, which consists of 10- and 20-ring openings viewed along the a and b directions (Fig. 5, right) and 8-ring openings viewed along the c-axis (Fig. 5, left), respectively. According to the categories by Kniep et al. [29], the title compound can be constructed by the fundamental building unit (FBU) $[B_2P_3O_{14}(OH)]$, which is composed of a $[B_2PO_9]$ 3-ring motif and two $P\Phi_4(\Phi=O, OH)$ tetrahedra, represented as $(5\,\square:\square<3\,\square>\square)$ (Fig. 5 inset). Up to present, several borophoshates have been reported to contain this FBU $(5\,\square:\square<3\,\square>\square)$. For examples, the loop-branched chain and the olB viewer-single layers from the condensation of such FBUs have been observed in a series of borophosphate compounds including $[Co(en)_3][B_2P_3O_{11}(OH)_2]$ [30], $Rb_2Co_3(H_2O)_2[B_4P_6O_{24}(OH)_2]$ [31] and $(C_2H_{10}N_2)M_{II}[B_2P_3O_{12}(OH)]$ (M_{II}=Mg, Mn–Zn, Cd) [32]. The title compound reported here is the first example with the 3D anionic partial structure built of this FBU $(5\,\square:\square<3\,\square>\square)$.

The anionic framework of the title compound is closely related to the series metal borophosphates $M^IM^{II}(H_2O)_2[BP_2O_8] \cdot yH_2O$ (M^I: Li, Na, K, Rb, Cs, NH4; M^{II}: Mn, Fe, Co, Ni, Cu, Zn, Cd; y: 0.2–1) **1** with helical ribbons of $^1_\infty\{[BP_2O_8]^{3-}\}$ [33,34] and $Zn_3(C_6H_{14}N_2)[B_6P_{12}O_{39}(OH)_{12}] \cdot (C_6H_{14}N_2)[HPO_4]$ **2** with an infinite mixed branched borophosphate chain $^1_\infty\{[B_6P_{12}O_{39}(OH)_{12}]^{12-}\}$ [35]. Considering the structural features, it can be found that all porous structures of these compounds can be described as the connectivity of two kinds of channels (type α and β) along the c-axis. The channel α is built of the spiral chains, and the channel β is formed by the connectivity of the adjacent chiral chains. It is worth noting that the size of such two channels could be changed regularly with the size augment of the fillers in channel β. For instance, the channel α is larger than the channel β in **1** because the filler in
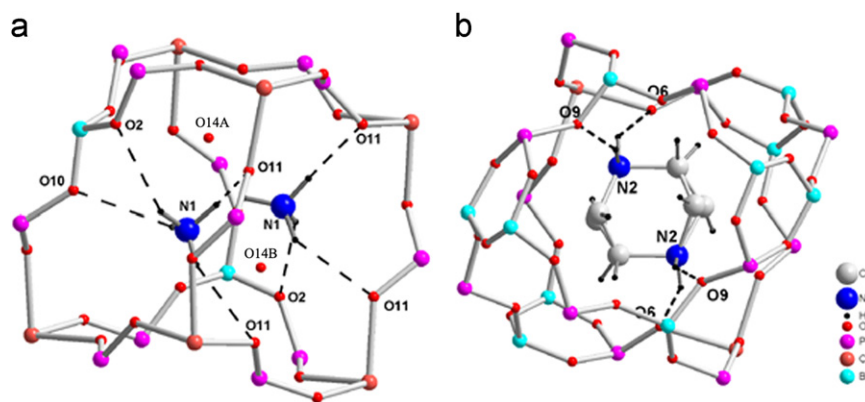
Fig. 4. Ball-and-stick side view of two types of cavities in the structure of the title compound: (a) the cavity built up from only eight-rings contains ammonium cations and water molecules and (b) the cavity built up from three- and eight-membered rings are occupied by a single dipronated piperazine cation.
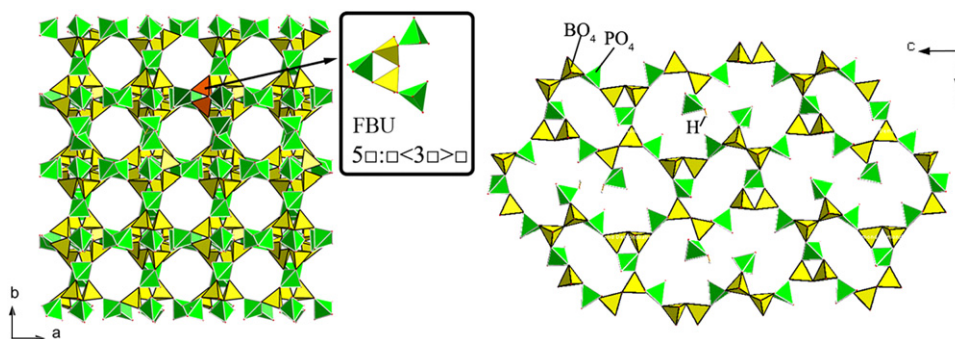

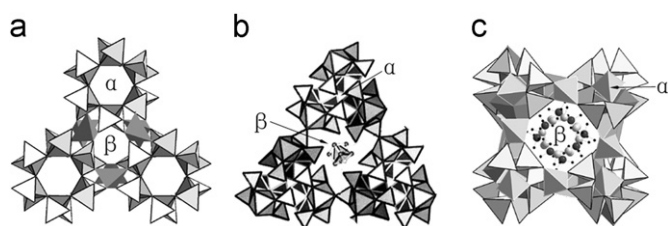**Fig. 5.** The 3-D borophosphate anionic partial structure of the title compound and its FBU.

Fig. 6. The size change of channels α and β in structural related borophosphates with the various templates, (a) $M^IM^{II}(H_2O)_2[BP_2O_8] \cdot yH_2O$ (M^I: Li, Na, K, Rb, Cs, NH$_4$; M^{II}: Mn, Fe, Co, Ni, Cu, Zn, Cd; y: 0.2–1), (b) $Zn_3(C_6H_{14}N_2)[B_6P_{12}O_{39}(OH)_{12}] \cdot (C_6H_{14}N_2)[HPO_4]$ and (c) $(NH_4)_2(C_4H_{12}N_2)[Co_2B_4P_6O_{24}(OH)_2]$.

channel β is only alkali metal cations (Fig. 6a), while the channel β enlarge with the introduction of the bigger organic templates. At the same time, the size of the channel α reduces obviously in **2** (Fig. 6b), and even disappear in the title compound (Fig. 6c). Therefore, it could be concluded that the templates have an important directing effect on the formation of the anionic structural topology of such borophosphates.

3.2. Magnetic characterization

The magnetic behavior of a microcrystalline sample of the title compound was studied in the magnetic field of 2 kOe (Fig. S4). At higher temperatures ($T > 50$ K) the sample is paramagnetic and obeys the Curie–Weiss law $\chi_m = \chi_0 + C/(T - \theta)$ with Curie–Weiss constants of $C = 2.69$ emu K/mol, and $\theta = -19.7$ K, respectively. The negative Weiss consistant implies that the weak antiferromagnetic ordering of the Co moments [36]. It is also confirmed by the

continuous decreasing of $\chi_m T$ on cooling. The sharp drop of the $\chi_m T$ value below 25 K could be caused by the combined effect of both the weak antiferromagnetic exchange and the zero-field splitting of the single Co(II) ion [37]. The effective magnetic moment per Co at 300 K is 4.77 μB, higher than the spin only value for spin $S = 3/2$ centers (3.87 μB), which might be attributed to the orbital contribution of Co(II) ions. Similar values have already been observed for the structural related cobalt(II) borophosphates [38,39].

4. Conclusions

A new organically-templated cobalt borophosphate, $(NH_4)_2(C_4H_{12}N_2)[Co_2B_4P_6O_{24}(OH)_2] \cdot H_2O$ with a novel borophosphate 3D anionic partial framework has been synthesized under mild hydrothermal conditions. It has a complex porous framework built of corner-sharing CoO$_6$ octahedra, BO$_4$ and PO$_4$ tetrahedra and an intersecting three-dimensional channel system, which is occupied by ammonium, dipronated piperazine ions and water molecules. The title compound is the first borophosphate compound with the 3D open framework containing the mixed cations. A comparison of the title compound with the structural related borophosphates shows the influence of the templates on the anionic structural topology. The magnetic susceptibilities for the title compound follow the Curie–Weiss law in a wide temperature range.

Appendix A. Supplementary material

Supplementary data associated with this article can be found in the online version at doi:10.1016/j.jssc.2011.07.032.

References

[1] A.K. Cheetham, G. Furey, T. Loiseau, Angew. Chem. Int. Ed. 38 (1999) 3268–3292.
[2] R. Murugavel, A. Choudhury, M.G. Walawalkar, R. Pothiraja, C.N.R. Rao, Chem. Rev. 108 (2008) 3549–3655.
[3] R. Kniep, G. Gözel, B. Eisenmann, C. Röhr, M. Asbrand, M. Kizilyalli, Angew. Chem. Int. Ed. Engl. 33 (1994) 749–751.
[4] R. Kniep, G. Schäfer, H. Engelhardt, I. Boy, H. Borrmann, Angew. Chem. Int. Ed. Engl. 38 (1999) 3641–3644.
[5] R.P. Bontchev, J. Do, A.J. Jacobson, Angew. Chem. Int. Ed. Engl. 38 (1999) 1937–1940.
[6] W. Liu, J.T. Zhao, Chin. J. Inorg. Chem. 19 (2003) 793–801.
[7] M. Yang, J.H. Yu, P. Chen, J.Y. Li, Q.R. Fang, R.R. Xu, Microporous Mesoporous Mater. 87 (2005) 124–132.
[8] W. Liu, M.R. Li, H.H. Chen, X.X. Yang, J.T. Zhao, Dalton Trans. (2004) 2847–2849.
[9] Y.X. Huang, B. Ewald, W. Schnelle, Y. Prots, R. Kniep, Inorg. Chem. 45 (2006) 7578–7580.
[10] T. Yang, G.B. Li, J. Ju, F.H. Liao, M. Xiong, J.H. Lin, J. Solid State Chem. 179 (2006) 2513–2519.
[11] X. Huang, O. Hochrein, D. Zahn, Y. Prots, H. Borrmann, R. Kniep, Chem. Eur. J. 14 (2007) 1737–1745.
[12] S.C. Sevov, Angew. Chem., Int. Ed. Engl. 35 (1996) 2630–2632.
[13] W. Liu, M.H. Ge, X.X. Yang, H.H. Chen, M.R. Li, J.T. Zhao, Inorg. Chem. 13 (2004) 3910–3914.
[14] E. Dumas, C. Debiemme-Chouvy, S.C. Sevov., J. Am. Chem. Soc. 124 (2002) 908–909.
[15] Y.X. Huang, W. Schnelle, H. Zhang, H. Borrmann, R. Kniep, J. Solid State Chem. 182 (2009) 920–924.
[16] T. Yang, G. Li, J. Ju, F.H. Liao, M. Xiong, J.H. Lin, J. Solid State Chem. 179 (2006) 2534–2540.
[17] R. Kniep, H. Engelhardt, C. Harf, Chem. Mater. 10 (1998) 2930–2934.
[18] M.R. Li, W. Liu, M.H. Ge, H.H. Chen, X.X. Yang, J.T. Zhao, Chem. Commun. (2004) 1272–1273.
[19] C. Hauf, R. Kniep, Z. Naturforsch. 52b (1997) 1432–1435.
[20] H.Y. Zhang, Z.X. Chen, L.H. Weng, Y.M. Zhou, D.Y. Zhao, Microporous Mesoporous Mater. 57 (2003) 309–316.
[21] D. Zhao, W.D. Cheng, H. Zhang, S.P. Huang, Z. Xie, W.L. Zhang, S.L. Yang, Inorg. Chem. 48 (2009) 6623–6629.
[22] H.Z. Xing, Y. Li, T. Su, J. Xu, W.T. Yang, E.B. Zhu, J.H. Yu, R.R. Xu, Dalton Trans. 39 (2010) 1713–1714.
[23] W.L. Zhang, W.D. Cheng, H. Zhang, L. Geng, Y.Y. Li, C.S. Lin, Z.Z. He, Inorg. Chem. 49 (2010) 2550–2556.
[24] W.T. Yang, J.Y. Li, Q.H. Pan, Z. Jin, J.H. Yu, R.R. Xu, Chem. Mater. 20 (2008) 4900–4905.
[25] T. Yang, J.L. Sun, G.B. Li, L. Eriksson, X.D. Zou, F.H. Liao, J.H. Lin, Chem. Eur. J 14 (2008) 7212–7217.
[26] W.T. Yang, J.Y. Li, T. Na, J. Xu, L. Wang, J.H. Yu, R.R. Xu, Dalton Trans. 40 (2011) 2549–2554.
[27] G.M. Sheldrick, SHELXS-97/2, Program for Solution of Crystal Structures, University of Göttingen, Germany, 1997;
G.M. Sheldrick, SHELXL-97/2, Program for Refinement of Crystal Structures, University of Göttingen, Germany, 1997.
[28] A.K. Cheetham, C.N.R. Rao, R.K. Fellera, Chem. Commun. (2006) 4780–4795.
[29] B. Ewald, Y.X. Huang, R. Kniep, Z. Anorg. Allg. Chem. 633 (2007) 1517–1540.
[30] S.C. Sevov, G.Y. Yang, Inorg. Chem. 40 (2001) 2214–2215.
[31] H. Engelhardt, W. Schnelle, R. Kniep, Z. Anorg. Allg. Chem. 626 (2000) 1380–1386.
[32] G. Schäfer, R. Kniep, Z. Anorg. Allg. Chem. 626 (2000) 141–147.
[33] R. Kniep, H.G. Will, I. Boy, C. Röhr, Angew. Chem., Int. Ed. 36 (1997) 1013–1014.
[34] M.H. Ge, J.X. Mi, Y.X. Huang, J.T. Zhao, R. Kniep, Z. Kristallogr. NCS 218 (2003) 165–166.
[35] G. Schäfer, W. Carrillo-Cabrera, S. Leoni, H. Borrmann, R. Kniep, Z. Anorg. Allg. Chem. 628 (2002) 67–76.
[36] Y.L. Zhou, M.H. Zeng, L.Q. Wei, B.W. Li, M. Kurmoo., Chem. Mater. 22 (2010) 4295–4303.
[37] S.S. Bao, L.M. Zheng, Y.J. Liu, W. Xu, S.H. Feng, Inorg. Chem. 42 (2003) 5037–5039.
[38] T. Yang, G.B. Li, J. Ju, F.H. Liao, M. Xiong, J.H. Lin, J. Solid State Chem. 179 (2006) 2534–2540.
[39] R.P. Bontchev, A.J. Jacobson, Mater. Res. Bull. 37 (2002) 1997–2005.